Molecular Crystals and Liquid Crystals
Publication details, including instructions for authors and subscription information:
http://www.tandfonline.com/loi/gmcl20

Optical Kerr Constant of Azo-Dye-Doped Nematic and Polymer-Dispersed Liquid Crystals Determined by Biphotonic Z-Scan Technique

Andy Ying-Guey Fuh [a] & Hui-Chi Lin [b]

[a] Department of Physics, Institute of Electro-Optical Science and Engineering, and Advanced Optoelectronic Technology Center, National Cheng Kung University, Tainan, Taiwan

[b] Department of Electro-Optical Engineering, and Institute of Electro-optical and Materials Science, National Formosa University, Huwei, Yunlin, Taiwan

Version of record first published: 30 Jun 2011

To cite this article: Andy Ying-Guey Fuh & Hui-Chi Lin (2011): Optical Kerr Constant of Azo-Dye-Doped Nematic and Polymer-Dispersed Liquid Crystals Determined by Biphotonic Z-Scan Technique, Molecular Crystals and Liquid Crystals, 541:1, 71/[309]-80/[318]

To link to this article: http://dx.doi.org/10.1080/15421406.2011.570151

Mol. Cryst. Liq. Cryst., Vol. 541: pp. 71/[309]–80/[318], 2011

ISSN: 1542-1406 print/1563-5287 online
DOI: 10.1080/15421406.2011.570151

Taylor & Francis
Taylor & Francis Group

Optical Kerr Constant of Azo-Dye-Doped Nematic and Polymer-Dispersed Liquid Crystals Determined by Biphotonic Z-Scan Technique

ANDY YING-GUEY FUH[1] AND HUI-CHI LIN[2]

[1]Department of Physics, Institute of Electro-Optical Science and Engineering, and Advanced Optoelectronic Technology Center, National Cheng Kung University, Tainan, Taiwan
[2]Department of Electro-Optical Engineering, and Institute of Electro-optical and Materials Science, National Formosa University, Huwei, Yunlin, Taiwan

We have recently investigated the optical Kerr constant (n_2) of azo-dye-doped nematic liquid crystal (ADDLC) and polymer-dispersed liquid crystal (ADDPDLC) films using the Z-scan technique. The measurements of ADDLC samples are firstly performed with the simultaneous application of two pump beams, which are referred as the biphotonic Z-scan technique. The results show that n_2 for ADDLC films is contributed primarily from the reorientation of liquid crystals induced by the photoisomerization of azo dyes and thermal effect, while that of ADDPDLC films with nano-sized LC droplets results from the thermal effect, and changes markedly with temperature.

Keywords Azo dyes; nematic liquid crystal; optical kerr constant; photoisomerization; polymer-dispersed liquid crystals; Z-scan

1. Introduction

Recently, azo-dye-doped liquid crystals (ADDLCs) have been extensively studied because of the increased nonlinearity of the host LC materials [1–3]. One important cause of such a high nonlinearity is the photo-induced reorientation of dye molecules. Based on this property, it has the potential for novel applications, such as displays [4,5], optical storage devices [6,7], holographic gratings [8,9], and other functions.

Among the known methods for measuring the nonlinearities of materials, Z-scan technique [10,11] is a simple but powerful technique for measuring optical Kerr constant (n_2) and nonlinear absorption coefficient (β) at the same time. The measurement of the optical Kerr constant is based on the principle of spatial beam distortion

Address correspondence to Andy Ying-Guey Fuh, Department of Physics, Institute of Electro-Optical Science and Engineering, and Advanced Optoelectronic Technology Center, National Cheng Kung University, Tainan 701, Taiwan. Tel.: +886-62757575x65228; Fax: +886-2747995; E-mail: andyfuh@mail.ncku.edu.tw

due to the self-focusing or self-defocusing that are associated with the intensity-dependent refractive index of the material. It has been applied to a wide range of materials [12–15]. We have recently studied the optical Kerr constants of azo-dye-doped nematic liquid crystal (ADDLC) [16,17] and polymer-dispersed liquid crystal (ADDPDLC) [18] films using the biphotonic Z-scan technique. Details of sample preparations, experiments, and results are described.

2. Experimental Methods

The nematic liquid crystal (NLC), photo-curable pre-polymer and azo dye used in this experiment are E7 (from Merck), NOA81 (from Norland Products) and disperse red 1 (DR1) (from Aldrich), D2 (from Sigma-Aldrich) or G239 (from Echo Chemical Co., Let.), respectively. The LC: azo dye mixing ratio of azo-dye-doped liquid crystals is 99:1 wt%. The mixing ratio of azo-dye-doped polymer-dispersed liquid crystals is 1 wt% G239, 24.75 wt% E7 and 74.25 wt% NOA81.

For the ADDLC samples, liquid crystals are aligned homogeneously. An empty cell having a cell-gap $\sim$15 μm or 25 μm is fabricated using two indium-tin-oxide (ITO)-coated glass plates, which are treated with polyvinyl alcohol (PVA) and rubbed to promote homogeneous alignment. The homogeneous azo dye-LCs mixture is then injected into an empty cell to form a homogeneously aligned azo-dye-doped liquid crystal film. The homogeneous alignment is verified using a conoscope.

To fabricate ADDPDLC samples, drops of the homogeneously mixed G239-E7-NOA81 compound are sandwiched between two pieces of ITO-coated glass without surface treatment. The cell gap of the ADDPDLC film is 12 μm thick. The filled ADDPDLC cell is finally polymerized under UV light with an intensity of $\sim$3 mW/cm^2. Figure 1 presents a side-view SEM image of the LC droplet morphology at the center of the ADDPDLC cell. The LC droplets are nano-sized, with sizes from $\sim$50 to 200 nm, which are smaller than the wavelength of visible light, such that the scattering of light by the LC droplets could be ignored.

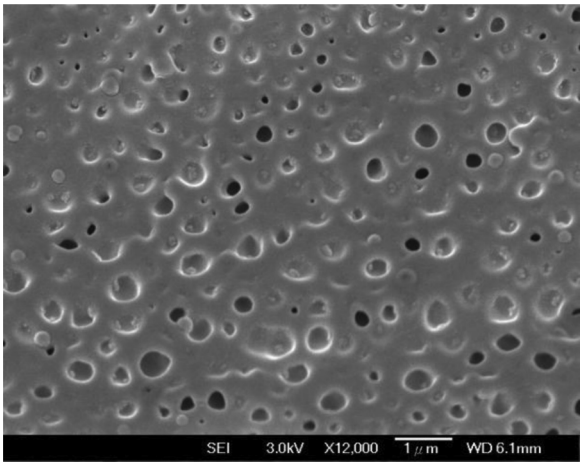

Figure 1. Side-view SEM image of droplet morphology at center of dye-doped nano-ADDPDLC cell.

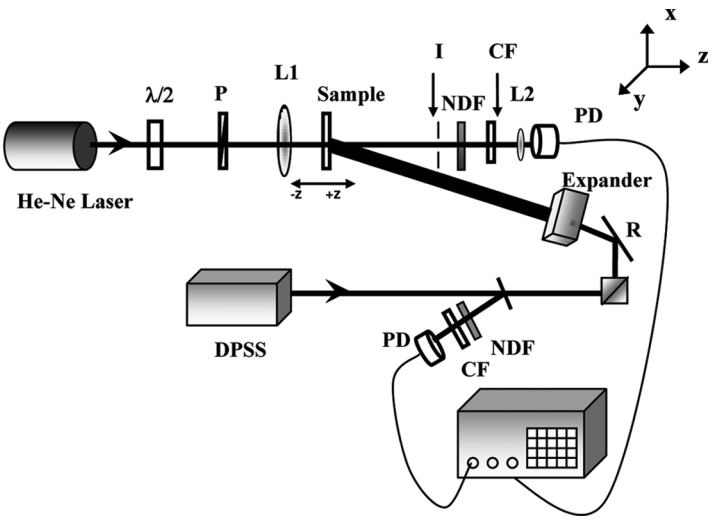

Figure 2. Red-beam-focused biphotonic Z-scan setup: P – polarizer; L – lens, I – iris; NDF – neutral density filter; CF – color filter; PBS – polarized beam splitter and PD – photodetector.

Figure 2 presents the red-light-focused biphotonic Z-scan setup. Light from a linearly polarized CW He-Ne laser ($\lambda = 633$ nm), propagating in the z direction, is focused onto a narrow waist beam with a lens that has a focal length of 6.5 cm. When required, a linearly polarized CW diode-pump solid state (DPSS) laser ($\lambda = 532$ nm) is simultaneously applied to the sample from its rear at an incident angle of $\sim 5^\circ$. The green light is expanded so that it irradiates the sample as it moves. The He-Ne and DPSS lasers are polarized parallel to the director of sample. The far-field transmitted intensity of the He-Ne beam is measured as a function of the sample position, using a photodetector placed behind a small iris.

Figure 3 presents the green-beam-focused biphotonic sequential Z-scan setup. A linearly polarized CW DPSS laser is focused by a lens with a focal length of 5 cm. When required, another linearly polarized CW diode laser ($\lambda = 670$ nm) is applied

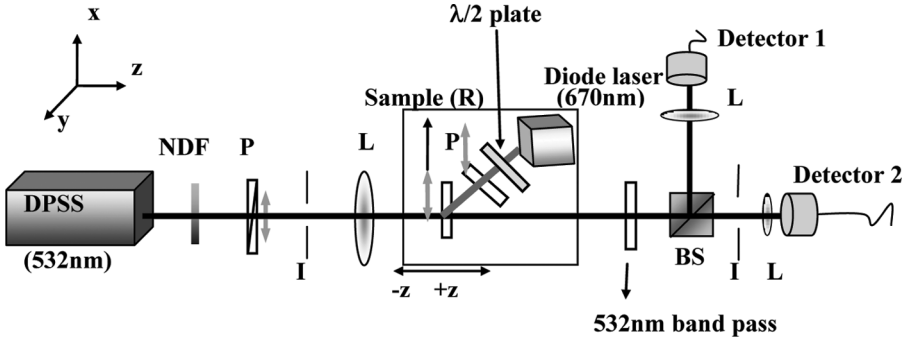

Figure 3. Green-beam-focused biphotonic Z-scan setup: DPSS – diode pumped solid state laser, NDF – neutral density filter, I – iris, L – lens, P – polarizer, BS – beam splitter. The diode laser, $\lambda/2$ plate, polarizer and the sample are arranged on the same stage, delineated by a square.

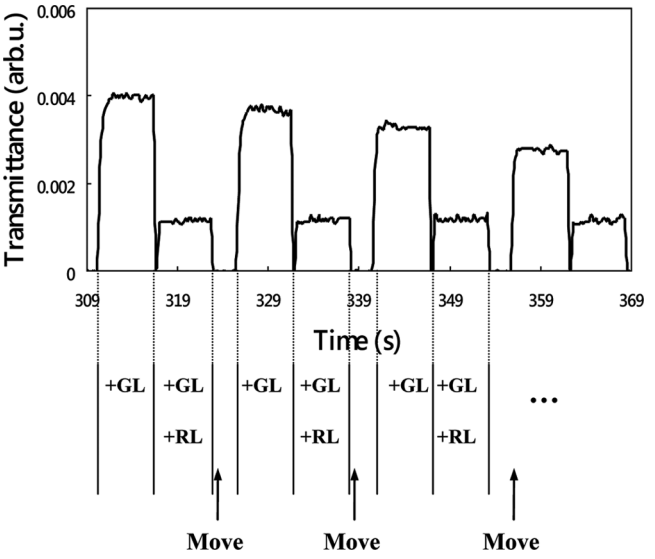

Figure 4. Sequential Z-scan measurements using the setup presented in Figure 3 made with detector 2. The sample is illuminated by green light from a DPSS laser (GL) only for 6 s initially, and then simultaneously illuminated by green light and red light (RL) from a diode laser for 6 s for a given sample location. Afterwards, the sample is moved through ~1 mm along the z-axis to the next location, and the measurements are repeated for 61 positions around the beam waist of the green laser.

to the sample from its rear side at an angle of incidence of ~25°. The variation of diode-laser intensity through the sample due to an oblique incidence with an angle of ~25° is calculated to be neglected. The DPSS and diode lasers are polarized parallel to the director of the sample. Notably, the red diode laser and the sample are arranged on a stage (the square box in Fig. 3) such that the laser can be moved as the sample is z-scanned by the green laser beam. Two lasers are applied to the sample in a special measurement sequence, which is called the sequential measurement as presented in Figure 4. Briefly, the sample is initially illuminated only by the green DPSS laser at each z-axis position for 6 s, and then is illuminated simultaneously with the green and red lasers for 6 s. The illuminations of the sample by green light only/green light and red light are repeated at sixty-one (61) z-axis positions near the beam waist of the DPSS laser.

3. Results and Discussion

3.1. *n_2 of ADDLC Films Measured Using Red-Light-Focused Biphotonic Z-Scan Technique*

Figure 5 presents the measured biphotonic Z-scan results for an ADDLC (1 wt% DR1 doped E7) sample (cell gap ~25 μm) using the setup shown in Figure 2. Notably, the intensity at the focus of the He-Ne laser is fixed at 2.5×10^6 mW/cm^2, as the intensity of the green light (I_G) is varied. Figure 5 shows that when a green light is applied simultaneously onto the sample, the Z-scan curve begins to vary. The peak-to-valley height $\Delta T_{p\text{-}v}$ initially increases with the green-light intensity to a maximum at $I_G = 98$ mW/cm^2, and then decreases to zero as the cross-dot curve

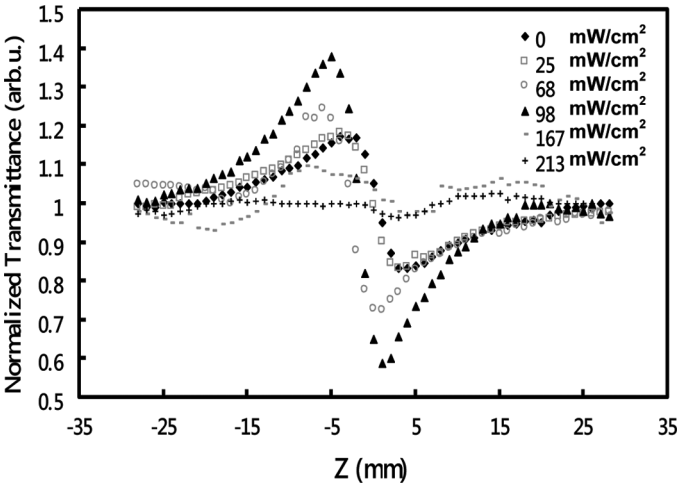

Figure 5. Variations of the Z-scan transmittance in a nematic liquid crystal film doped with 1% azo-dye (DR1) with various intensities of green light. The curves are normalized with the transmittance measured at a point far behind the focus point.

shown in Figure 5. Notably, the Z-scan measurements of ADDLC samples are firstly performed with the simultaneous application of two pump beams, which are the so-called biphotonic Z-scan technique.

From the peak-to-valley height ($\Delta T_{p\text{-}v}$) of the curves shown in Figure 5, the optical Kerr constant can be determined [10,11] using the equation,

$$\Delta T_{p\text{-}v} \cong 0.406(1-S)^{0.25}\Delta\Phi_0, \tag{1}$$

where $S \sim 0.4$ is the linear transmittance of the iris and $\Delta\Phi_0$ is the phase distortion. The phase distortion is defined as $\Delta\Phi_0 = 2\pi L_{eff}\Delta n_0/\lambda$, where $L_{eff} = (1 - e^{-\alpha L})/\alpha$, where α and L are the linear absorption coefficient and the thickness of the sample, respectively. The on-axis change in the index at the focus, Δn_0, is linearly related to the optical Kerr constant n_2 by

$$\Delta n_0 = n_2 I_0, \tag{2}$$

where I_0 is the intensity of the laser beam at the focal point. Equations (1) and (2) demonstrate that n_2, are $-1.74 \times 10^{-6}\,cm^2/W$, $-1.76 \times 10^{-6}\,cm^2/W$, $-2.61 \times 10^{-6}\,cm^2/W$ and $-3.96 \times 10^{-6}\,cm^2/W$ when I_G is set to 0, 25, 68 and 98 mW/cm^2, respectively.

For the ADDLC sample illuminated with red light only, the nonlinearity is believed to arise from the thermal effect induced by the absorption of light by dye. Since the He-Ne laser is a Gaussian beam, the central region of the illuminated spot in the sample is hotter than the outer region. Besides, the polarization of the He-Ne laser is parallel to the LC director axis. The temperature-dependent refractive index of a typical nematic LC elucidates that the central region of the illuminated spot has a smaller refractive index than the outer region. Therefore, a de-focusing effect is observed, meaning that n_2 is negative.

When a green light is applied simultaneously onto the sample, n_2 initially increases with the green-light intensity. As I_G increases further, $\Delta T_{p\text{-}v}$ decreases. The variation of $|n_2|$ with the additional irradiation of green light is believed to be caused by the thermal effect. Because the expanded green beam induces the temperature of the whole illuminated spot to increase, the difference between the refractive indices in the central and outer regions increases, and $|n_2|$ becomes larger. The maximum measured value of n_2 is $-3.96 \times 10^{-6}\,cm^2/W$ at $I_G = 98\,mW/cm^2$. However, as I_G increases further, the temperature of the illuminated spot approaches the clear temperature (T_C) of the sample, a chaotic Z-scan curve is observed. When the green-beam intensity reaches a critical value, such that the temperature of the irradiated spot equals or exceeds T_C, the Z-scan curve becomes a horizontal straight line. (See the cross-dot curve in Figure 5.)

Figure 6 plots the dynamic Z-scan measurements when a green light is applied with $I_G = 98\,mW/cm^2$. Curves (a) and (b) are the transmittances at the peak and valley points in the diamond-dot curve in Figure 5 (without the irradiation of green light), respectively. When the green light is turned on, $\Delta T_{p\text{-}v}$ becomes smaller transiently, meaning that the transmittance at the peak point decreases, while the transmittance at the valley point increases. The cause is believed to be due to the photoisomerization effect, which induces LC reorientation. Immediately after the green light is turned on, the green light induces photoisomerization of azo dyes from the trans form to cis form, while the red light induces the inverse transformation by photoisomerization, which are referred as the biphotonic effect. When dye molecules are transformed to the cis form, they become bent in molecular structure, and in turn, induce reorientation of liquid crystals with their director axis perpendicular to the polarization of the green laser. Because of the biphotonic effect, the change of refractive index in the central region of the spot illuminated by the strong red-light is smaller than the corresponding change in the outer region (where the red light was weak). Thus, de-focusing effect is suppressed. At this time, n_2 decreases to $-1.39 \times 10^{-6}\,cm^2/W$ from $-1.74 \times 10^{-6}\,cm^2/W$. As the green light continues to be applied, the thermal effect gradually strengthens, and eventually dominates.

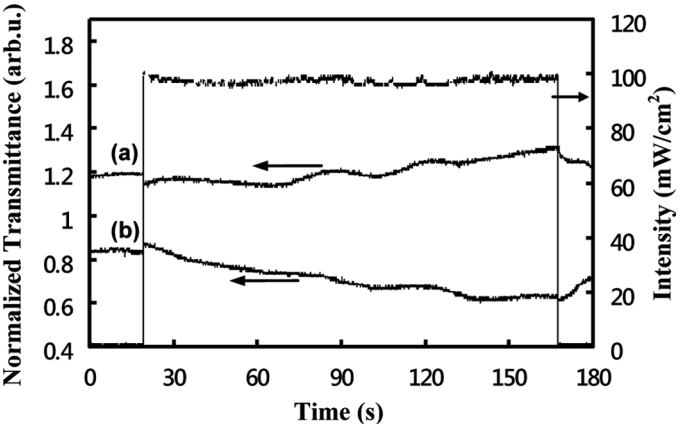

Figure 6. Effects of dynamic Z-scan when green light is applied ($98\,mW/cm^2$). Curves (a) and (b) are the transmittances at the two positions, at which the transmittances are maximal and minimal when no green light is applied.

Therefore, $\Delta T_{p\text{-}v}$ increases, that agrees with the results shown in Figure 5. Finally, when the green light is switched off, $\Delta T_{p\text{-}v}$ decreases, and eventually returns to its original value.

3.2. *Measurements of n_2 of ADDLC Films Using Green-Light-Focused Biphotonic Sequential Z-Scan Technique*

In the present biphotonic experiment, the optical Kerr constant of 1 wt% D2-doped liquid crystal film (15 μm thick) is measured using the sequential biphotonic Z-scan setup shown in Figure 3. The experiments are performed by using the sequential measurement (Fig. 4) with various red-light intensities keeping the green light power at 0.7 mW. Figure 7 plots the absolute value of measured n_2. Notably, the open-diamond-dot curve displays n_2 of the cell illuminated with green light only, and the solid-square-dot curve gives n_2 of the cell illuminated with green and red light simultaneously. In Figure 7, $|n_2|$ of the cell that is illuminated with green light only remains approximately constant at $\sim 8.25 \times 10^{-3}\,cm^2/W$, while that of the cell illuminated simultaneously with red light increases with the intensity of red light (I_R). The value of $|n_2|$ peaks with $\sim 1.65 \times 10^{-2}\,cm^2/W$ at $I_R \sim 1.8\,W/cm^2$, before decreasing and finally increasing slightly again. These results can be understood as follows.

When an ADDLC cell is illuminated using a DPSS green laser only, the excited dyes are reoriented with their long axes along the direction perpendicular to the polarization of DPSS laser due to photoisomerization effect. Because the DPSS laser polarized parallel to the LC director is a Gaussian beam, the central region of the illuminated spot "sees" a smaller refractive index than the outer region. Thus, a self-defocusing effect is observed.

When the sample is illuminated simultaneously by green and red light, the biphotonic process (trans→cis and cis→trans photoisomerizations) results in a

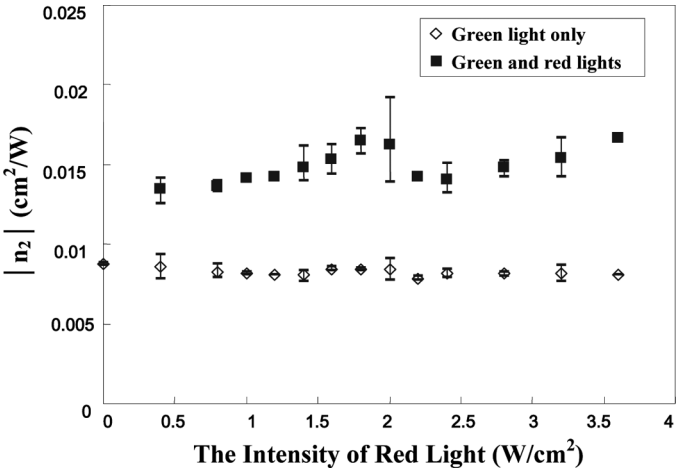

Figure 7. Measured the optical Kerr constant $|n_2|$ when an ADDLC cell is illuminated only with green light, and with both red and green light, as a function of the intensity of the red light. The results are obtained using the sequential measurement method that is presented in Figure 4.

higher concentration of trans-isomers than that is illuminated with green light only, and then LCs tends to remain in their original direction. Therefore, for an ADDLC cell that is illuminated simultaneously with green light (I_G) and red light (I_R) having an intensity ranging from 0.4 to 1.8 W/cm^2, the match between I_R and I_G in the outer region of the illuminated spot increases with I_R. Consequently, the gradient of the refractive index (defocusing effect) seen by the green light increases as well with I_R. $|n_2|$ resulted from such an intensity matching in the outer region of the illuminated spot is maximized at $I_R \sim 1.8$ W/cm^2. In the region of $I_R = 1.8$–2.4 W/cm^2, the strong red light induces re-orientation of more LC molecules in the central region of the illuminated spot parallel to the polarization of the green light due to the biphotonic effect. The defocusing effect of the sample thus decreases.

The value of $|n_2|$ would decrease continuously as I_R increases above 2.4 W/cm^2, if only the biphotonic effect applies. However, the results in Figure 7 reveal that $|n_2|$ increases slightly with I_R above 2.4 W/cm^2. The cause is attributed to the thermal effect, which compensates for the molecular reorientation nonlinearity of the sample at high red-light intensity. The average temperature of the illuminated region simultaneously with a red light and a green light in the sample is measured using a handy thermo TVS-200EX to verify the thermal effect, which contributes a defocusing increasing with I_R.

Notably, the open-diamond-dot curve in Figure 7, which is obtained with the sample illuminated only with green light, is almost a straight line. As mentioned above, the ADDLC sample is measured by a sequential Z-scan technique (Fig. 4), i.e., the sample is illuminated by a focused green laser only, and then simultaneously with a linearly polarized homogeneous red light. It indicates that the defocusing effect of the sample caused by only green light does not be altered by biphotonic illumination.

3.3. *n_2 of ADDPDLC Films with Nano-Sized LC Droplets Measured Using Z-Scan Technique*

In this part, the optical Kerr constants of ADDPDLC (1 wt% G239 + 24.75 wt% E7 + 74.25 wt% NOA81) films with nano-sized LC droplets are measured using Z-scan technique. The setup is similar to that shown in Figure 3, but the diode laser is moved. Figure 8 plots the calculated temperature-dependent optical Kerr constants for the ADDPDLC film. The results indicate that the nonlinearity of an ADDPDLC film changes markedly with temperature. n_2 increases with temperature to a peak value of $\sim -2.96 \times 10^{-3}$ cm^2/W at 35°C, before decreasing finally to approximately a constant of $\sim -1.13 \times 10^{-3}$ cm^2/W. The causes of such temperature-dependent results in an ADDPDLC film are as follows.

Liquid crystals are birefringent. The refractive index of LCs in the droplets equals the average refractive index $n_a \sim (n_e + 2n_o)/3$, where n_e and n_o are the extra-ordinary and ordinary refractive index, respectively. The variation of n_a with temperature is similar to that of n_e. Therefore, the LC droplets in the ADDPDLC film contribute a defocusing effect due to thermal effect. As the ambient temperature increases, the difference between the refractive indices in the central and outer regions of the illuminated spot increases, and the defocusing effect therefore increases. The maximum defocusing effect, $n_2 = -2.96 \times 10^{-3}$ cm^2/W, is observed at 35°C, and then n_2 decreases steeply in 40°C. This phenomenon is due to the decrease in the clearing temperature of the sample. A power-compensation differential scanning calorimeter

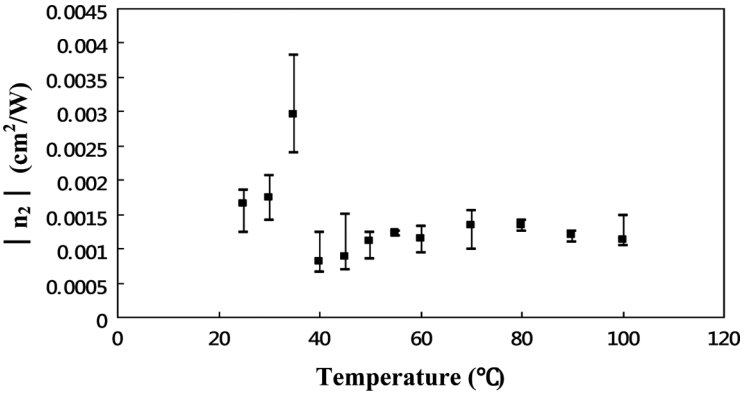

Figure 8. Variation of measured optical Kerr constant n_2 for ADDPDLC film with temperature.

(DSC) is adopted to measure the phase transition temperatures of the materials. The clearing temperatures of liquid crystal E7 and ADDPDLC films are found to be 61°C and 43.08°C, respectively.

When the temperature exceeds 40°C, the liquid crystals in the central and outer regions of the illuminated spot are isotropic, and confirmed with the use of a DSC measurement. The optical Kerr constants at these temperatures are $\sim -1.13 \times 10^{-3}\,\mathrm{cm}^2/\mathrm{W}$. This defocusing effect is caused by the polymer density gradient in the illuminated region due to the thermal effect induced by the azo dye absorbing the laser light.

4. Conclusions and Perspectives

We have presented n_2 of azo-dye-doped nematic and polymer-dispersed liquid crystals determined by biphotonic Z-scan technique. The results demonstrate that n_2 of ADDLC films measured using Z-scan technique with a red beam can be modulated and/or switched by applying a green light laser. When green light is simultaneously applied to the sample, the photoisomerization effect is observed transiently. Using the green-beam-focused biphotonic sequential Z-scan, the variation of n_2 of ADDLC samples indicates that the molecular reorientation of the liquid crystals induced by the photoisomerization of the azo dyes dominates at low red-light intensity, but thermal effect compensates for the molecular reorientational nonlinearity of the sample at high red-light intensity. Besides, n_2 of the ADDPDLC film with nano-sized LC droplets can be changed by varying the sample temperature.

Acknowledgment

The authors would like to thank the National Science Council of the Republic of China (Taiwan) for financially supporting this research under the Grant No. NSC 98-2112-M-006-011-MY3. Additionally, this work is partially supported by Advanced Optoelectronic Technology Center.

References

[1] Becchi, M., Jánossy, I., Shankar Rao, D. S., & Statman, D. (2004). *Phys. Rev. E*, *69*, 051707.

[2] He, Tingchao, Cheng, Yongguang, Du, Yabing & Mo, Yujun (2007). *Opt. Comm.*, *275*, 240.

[3] Rodríguez-Rosales, A. A., Morales-Saavedra, O. G., Román-Moreno, C. J., & Ortega-Martínez, R. (2008). *Opt. Mat.*, *31*, 305.

[4] Lin, Tsung-Hsien, Jau, Hung-Chang, Hung, San-Yi, Fuh, Huei-Ru, & Fuh, Andy Y.-G. (2006). *Appl. Phys. Lett.*, *89*, 021116.

[5] Cheng, Ko-Ting, Liu, Cheng-Kai, Ting, Chi-Lun & Fuh, Andy Ying-Guey (2008). *Opt. Comm.*, *281*, 5133.

[6] Wu, Wei-Yen & Fuh, Andy Ying-Guey (2007). *Jpn. J. Appl. Phys.*, *46*, 6761.

[7] Fei, Haosheng, Wei, Zhenqian, Wu, Pengfei, Han, Li, Zhao, Yingying, & Che, Yanlong (1994). *Opt. Lett.*, *19*, 411.

[8] Lee, C.-R., Mo, T.-S., Cheng, K.-T., Fu, T.-L., & Fuh, A. Y.-G. (2003). *Appl. Phys. Lett.*, *83*, 4285.

[9] Fuh, A. Y.-G., Liao, C.-C., Hsu, K.-C., & Lu, C.-L. (2003). *Opt. Lett.*, *28*, 1179.

[10] Sheik-Bahae, M., Said, A. A., & Van Stryland, E. W. (1989). *Opt. Lett.*, *14*, 955.

[11] Sheik-Bahae, M., Said, A. A., Wei, T. H., Hagan, D. J., Van Stryland, E. W. (1990). *IEEE J. Quantum Electron.*, *26*, 760.

[12] Kosa, T., & Janossy, I. (1995). *Opt. Lett.*, *20*, 1230.

[13] Alves, S., Sant'Anna Cuppo, F. L., Bourdon, A., & Figueiredo Neto, A. M. (2006). *J. Opt. Soc. Am. B*, *23*, 2328.

[14] Santos, M. P., Gómez, S. L., Bringuier, E., & Figueiredo Neto, A. M. (2008). *Phys. Rev. E*, *77*, 011403.

[15] Esteves, J., & Figueiredo Neto, A. M. (2002). *Liq. Cryst.*, *29*, 733.

[16] Fuh, Andy Ying-Guey, Lin, Hui-Chi, Mo, Ting-Shan, & Chen, Ching-Hsu (2005). *Opt. Express*, *13*, 10634.

[17] Lin, Hui-Chi, Wang, Jyun-Ruie, Wu, Wei-Yen, & Fuh, Andy Y.-G. (2008). *Opt. Comm.*, *281*, 3183.

[18] Lin, Hui-Chi, Chen, Chin-Hui, Mo, Ting-Shan, Hsieh, Feng-Ming, Lui, Jui-Hsiang, & Fuh, Andy Ying-Guey (2010). *Opt. Comm.*, *283*, 323.